# Kinematic Analysis and Design of a New 3-DOF Translational Parallel Manipulator

**Yangmin Li**
e-mail: ymli@umac.mo

**Qingsong Xu**
e-mail: ya47401@umac.mo

Department of Electromechanical Engineering,
Faculty of Science and Technology,
University of Macau,
Av. Padre Tomás Pereira S.J.,
Taipa, Macao SAR, China

*A new three degrees of freedom (3-DOF) translational parallel manipulator (TPM) with fixed actuators called a 3-PRC TPM is proposed in this paper. The mobility of the manipulator is analyzed via screw theory. The inverse kinematics, forward kinematics, and velocity analysis are performed and the singular and isotropic configurations are identified afterward. Moreover, the mechanism design to eliminate all singularities and generate an isotropic manipulator has been presented. With the variation on architectural parameters, the reachable workspace of the manipulator is generated and compared. Especially, it is illustrated that the manipulator in principle possesses a uniform workspace with a constant hexagon shape cross section. Furthermore, the dexterity characteristics are investigated in the local and global sense, respectively, and some considerations for real machine design have been proposed as well.* [DOI: 10.1115/1.2198254]

*Keywords: parallel manipulators, mechanism design, kinematics, singularity, isotropy, workspace, dexterity*

## 1 Introduction

In recent years, the progress in the development of parallel manipulators (PMs) has been accelerated since PMs possess many advantages over their serial counterparts in terms of high accuracy, velocity, stiffness, and payload capacity, therefore allowing their wide range of applications as industrial robots, flight simulators, micromanipulators, and parallel machine tools, etc. However, the most notable drawback of parallel manipulators is their relatively limited workspace.

A parallel manipulator typically consists of a mobile platform that is connected to a fixed base by several limbs or legs in parallel. An exhaustive enumeration of parallel robots' mechanical architectures and their versatile applications are described in [1]. Most six degrees of freedom (6-DOF) parallel manipulators are based on the Gough-Stewart platform architecture due to the advantages mentioned above. However, 6-DOF is not necessarily required in many situations.

Therefore, in recent years, the limited-DOF manipulators that both maintain the inherent advantages of parallel mechanisms and possess several other advantages in terms of the total cost reduction in manufacturing and operations, are attracting the attention of various researchers [2–4]. Many spatial 3-DOF parallel manipulators have been designed and investigated for relevant applications, such as the famous DELTA robot with three translational DOF whose concept then has been realized in many different configurations [5], the Orthoglide parallel robot with pure translational DOF [6], spherical 3-DOF mechanisms with pure rotational motions, and (3-PRS) parallel manipulators with mixed DOF [7–9], etc.

Among these architectures, translational parallel manipulators (TPMs) have a potentially wide range of applications that need a pure translational motion in case of a motion simulator, a positioning tool of an assembly line, and others. Several other types of architectures have been proposed to achieve pure translational motions with different theoretical approaches, like the (3-UPU) platform [10], (3-RUU), (3-PUU) mechanisms [11], (3-RPC) architecture [12], (3-CRR) manipulator [13,14], etc. Here the notation of R, P, U, C, and S denote the revolute, prismatic, universal, cylindrical, and spherical joint, respectively.

In this paper, a new type of manipulator with 3-PRC topology actuated by fixed actuators is proposed to achieve three pure translational DOF. The fixed actuators make it possible that the moving components of the manipulator do not bear any loads of the actuators. This enables large powerful actuators to drive relatively small structures in order to facilitate the design of manipulators with faster, stiffer, and stronger characteristics. Additionally, being an overconstrained mechanism, the proposed 3-PRC TPM is constructed using fewer links and joints than it is expected, and possesses a much simpler structure than most of the existed TPMs, that leads to an extensive reduction in cost and complexity of the device. To the knowledge of the authors, the described 3-PRC TPM never appeared before in either academia or industry.

The remainder of the paper is organized as follows. After a short description of the kinematic architecture, the mobility of the manipulator is analyzed via screw theory in Sec. 2. The inverse and forward kinematics solutions are derived in closed form in Sec. 3, and the velocity analysis is performed in Sec. 4. Then in Sec. 5, the singular configurations are identified and the methods to eliminate them are proposed. In addition, the isotropic configurations are derived in Sec. 6. For a real machine design, it is also necessary to determine how the kinematic features vary with the changing of architectural parameters. Motivated by this, with the variations of the mobile platform size and actuators layout angle, the workspace is generated and compared in Sec. 7, and the dexterity analysis of the manipulator is performed in detail in Sec. 8. Finally, some concluding remarks involving design considerations are given in Sec. 9.

## 2 Description and Mobility Analysis of the Manipulator

**2.1 Architecture Description.** The computer aided design (CAD) model and schematic diagram of a 3-PRC TPM is shown in Figs. 1 and 2, respectively. It consists of a mobile platform, a fixed base, and three limbs with identical kinematic structure. Each limb connects the fixed base to the mobile platform by a P joint, a R joint, and a C joint in sequence, where the P joint is

Contributed by the Mechanics and Robotics Committee of ASME for publication in the JOURNAL OF MECHANICAL DESIGN. Manuscript received January 28, 2005; final manuscript received September 5, 2005. Review conducted by Hashem Ashrafiuon. Paper presented at the IEEE International Conference on Robotics & Automation (ICRA), 2005.

 Copyright © 2006 by ASME 

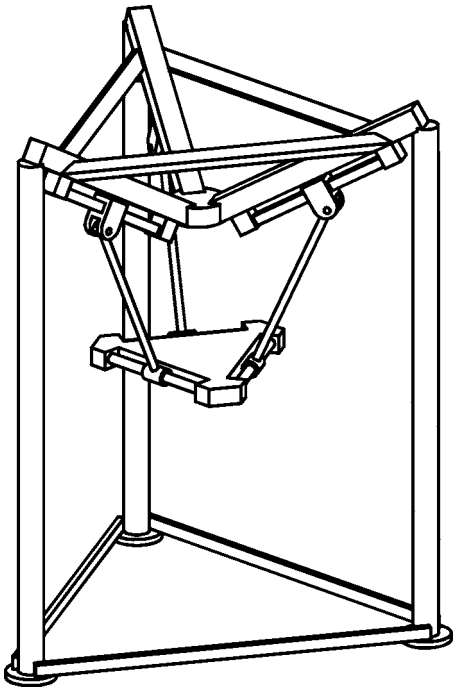

**Fig. 1 A 3-PRC translational parallel manipulator**

driven by a linear actuator assembled on the fixed base. Thus, the mobile platform is attached to the base by three identical PRC linkages. The following mobility analysis shows that in order to keep the mobile platform from changing its orientation, it is sufficient for the three axes of joints within the same limb to satisfy some certain geometric conditions. That is, (i) the R joint axis ($\mathbf{r}_i$) and C joint axis ($\mathbf{c}_i$) within the $i$-th limb, for $i=1$, 2, and 3, are parallel to the same unit vector $\mathbf{s}_{i0}$, and (ii) the limbs are arranged so that $\mathbf{s}_{i0} \neq \mathbf{s}_{j0}$ for $i \neq j$, and $i$, $j=1$, 2, and 3.

**2.2 Mobility Analysis.** The general Grübler-Kutzbach criterion is useful in mobility analysis for many parallel manipulators, however it is difficult to apply this criterion directly to mobility analysis of overconstrained limited-DOF parallel manipulators. For example, the number of DOF of a 3-PRC TPM given by the general Grübler-Kutzbach criterion is

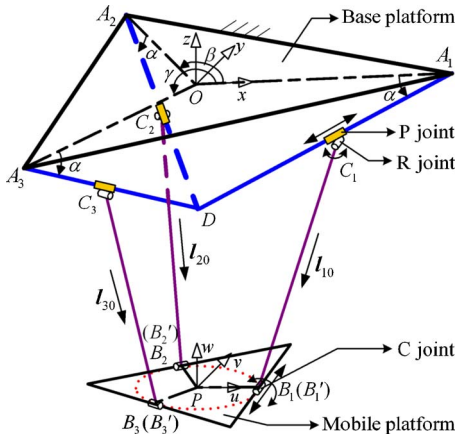


**Fig. 2 Schematic representation of a 3-PRC TPM**

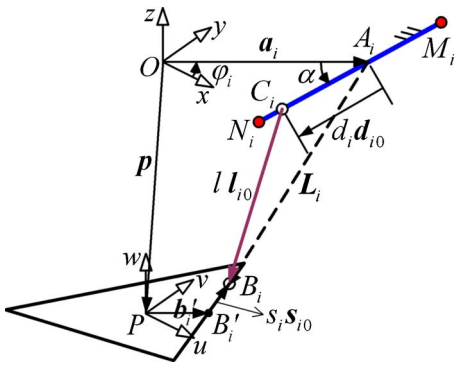

**Fig. 3 Geometry of one typical kinematic chain**

$$F = \lambda(n - j - 1) + \sum_{i=1}^{j} f_i = 6(8 - 9 - 1) + 12 = 0 \qquad (1)$$

where $\lambda$ represents the dimension of task space, $n$ is the number of links, $j$ is the number of joints, and $f_i$ denotes the degrees of freedom of joint $i$.

Another drawback of the general Grübler-Kutzbach criterion is that it can only derive the number of DOF of some mechanisms but cannot obtain the properties of the DOF, i.e., whether they are translational or rotational DOF.

On the contrary, we can effectively analyze the mobility of a 3-PRC TPM by resorting to screw theory [4]. For a limited-DOF parallel manipulator, the motion of each limb that can be treated as a twist system is guaranteed under some exerted structural constraints which are termed as a wrench system. The wrench system is a reciprocal screw system of the twist system for the limb, and a wrench is said to be reciprocal to a twist if the wrench produces no work along the twist. The mobility of the manipulator is then determined by the combined effect of wrench systems of all limbs.

For a 3-PRC TPM, the twist system for each limb is a four-order screw system, and it is not difficult to derive the wrench system that is a reciprocal screw system of order 2 which exerts two constraint couples to the mobile platform with their axes perpendicular to the axis of the R joint. The wrench system of the mobile platform, that is a linear combination of wrench systems of all the three limbs, is a system of order 3 because the three wrench systems of order 2 consist of six couples which are linearly dependent and form a screw system of order 3. Since the direction of each R joint axis satisfies the conditions described above, i.e., it is invariable, the wrench systems restrict three rotations of the mobile platform with respect to the fixed base at any instant. Thus leads to a translational parallel manipulator.

## 3 Kinematic Modeling

**3.1 Inverse Kinematic Modeling.** The purpose of the inverse kinematics issue is to solve the actuated variables from a given position of the mobile platform.

To facilitate the analysis, as shown in Figs. 2 and 3, we assign a fixed Cartesian frame $O\{x,y,z\}$ at the centered point $O$ of the fixed base, and a moving Cartesian frame $P\{u,v,w\}$ on the triangle mobile platform at the centered point $P$, with the $z$ and $w$ axes perpendicular to the platform, and the $x$ and $y$ axes parallel to the $u$ and $v$ axes, respectively.

In addition, the $i$-th limb $C_iB_i$ ($i=1,2,3$) with the length of $l$ is connected to the mobile platform at point $B_i$ which is a point on the axis of the $i$-th C joint. $B_i'$ denotes the point on the mobile platform that is coincident with the initial position of $B_i$, and the three points $B_i'$ for $i=1$, 2, and 3 lie on a circle of radius $b$. The three rails $M_iN_i$ intersect each other at point $D$ and intersect the $x$-$y$ plane at points $A_1$, $A_2$, and $A_3$ that lie on a circle of radius $a$.

The sliders of P joints $C_i$ are restricted to move along the rails between $M_i$ and $N_i$. Moreover, the axis of the P joint is perpendicular to the axes of R and C joints within the $i$-th limb. Angle $\alpha$ is measured from the fixed base to rails $M_iN_i$ and is defined as the layout angle of actuators. In order to obtain a compact architecture, the value of $\alpha$ is designed within the range of [0 deg, 90 deg]. Angle $\varphi_i$ is defined from the $x$ axis to $\overrightarrow{OA_i}$ in the fixed frame, and also from the $u$ axis to $\overrightarrow{PB'_i}$ in the moving frame. Without losing generality, let the $x$-axis point along $\overrightarrow{OA_1}$, and the $u$-axis direct along $\overrightarrow{PB'_1}$. Then, we have $\varphi_1=0$ deg. Additionally, let $d_{\max}$ and $s_{\max}$ denote the maximum stroke of linear actuators and C joints, respectively, i.e.,

$$-\frac{d_{\max}}{2} \leqslant d_i \leqslant \frac{d_{\max}}{2} \tag{2}$$

$$-\frac{s_{\max}}{2} \leqslant s_i \leqslant \frac{s_{\max}}{2} \tag{3}$$

for $i=1$, 2, and 3.

As shown in Fig. 3, the position vectors of points $A_i$ and $B'_i$ with respect to frames $O$ and $P$, respectively, can be written as ${}^O\mathbf{a}_i$ and ${}^P\mathbf{b}'_i$, where a leading superscript indicates the coordinate frame with respect to which a vector is expressed. For brevity, the leading superscript will be omitted whenever the coordinate frame is the fixed frame, e.g., $\mathbf{a}_i={}^O\mathbf{a}_i$. Generally, the position and orientation of the mobile platform with respect to the fixed frame can be described by a position vector $\mathbf{p}=[p_x\ p_y\ p_z]^T=\overrightarrow{OP}$, and a $3\times3$ rotation matrix ${}^O\mathbf{R}_P$. Since the mobile platform of a 3-PRC TPM possesses only a translational motion, ${}^O\mathbf{R}_P$ becomes an identity matrix. Then, we have $\mathbf{b}'_i={}^P\mathbf{b}'_i$.

Referring to Fig. 3, a vector-loop equation can be written for the $i$-th limb as follows:

$$l\mathbf{l}_{i0}=\mathbf{L}_i-d_i\mathbf{d}_{i0} \tag{4}$$

with

$$\mathbf{L}_i=\mathbf{p}+\mathbf{b}'_i+s_i\mathbf{s}_{i0}-\mathbf{a}_i \tag{5}$$

where $\mathbf{l}_{i0}$ is the unit vector along $\overrightarrow{C_iB_i}$, $d_i$ represents the linear displacement of the $i$-th actuated joint, $\mathbf{d}_{i0}$ is the unit vector directing along rail $M_iN_i$, $s_i$ is the stroke of the $i$-th C joint, and $\mathbf{s}_{i0}$ denotes the unit vector parallel to the axes of the C and R joints of limb $i$, which can be derived by

$$\mathbf{s}_{i0}=[-s\varphi_i\quad c\varphi_i\quad 0]^T \tag{6}$$

where $c$ stands for cosine, and $s$ stands for sine.

Substituting Eq. (5) into Eq. (4) and dot-multiplying both sides of the expression by $\mathbf{s}_{i0}$ allows the derivation of $s_i$, i.e.,

$$s_i=-\mathbf{s}_{i0}^T\mathbf{p} \tag{7}$$

Dot-multiplying Eq. (4) with itself and rearranging the items, yields

$$d_i^2-2d_i\mathbf{d}_{i0}^T\mathbf{L}_i+\mathbf{L}_i^T\mathbf{L}_i-l^2=0 \tag{8}$$

Solving Eq. (8), leads to solutions for the inverse kinematics problem

$$d_i=\mathbf{d}_{i0}^T\mathbf{L}_i\pm\sqrt{(\mathbf{d}_{i0}^T\mathbf{L}_i)^2-\mathbf{L}_i^T\mathbf{L}_i+l^2} \tag{9}$$

It can be observed that there exist two solutions for each actuated variable, hence there are totally eight possible solutions for a given mobile platform position. To enhance the stiffness of the manipulator, only the negative square root in Eq. (9) is selected in this paper to yield a unique solution where the three legs are inclined inward from top to bottom.

**3.2 Forward Kinematic Modeling.** Given a set of actuated inputs, the position of the mobile platform can be solved by the forward kinematic analysis.

In view of Eqs. (4) and (5), we can derive that

$$\mathbf{p}+s_i\mathbf{s}_{i0}-\mathbf{e}_i=l\mathbf{l}_{i0} \tag{10}$$

where

$$\mathbf{e}_i=\mathbf{a}_i+d_i\mathbf{d}_{i0}-\mathbf{b}'_i=[e_{ix}\quad e_{iy}\quad e_{iz}]^T \tag{11}$$

Dot-multiplying Eq. (10) with itself and considering Eqs. (6), (7), and (11), yields

$$(p_xc^2\varphi_i+p_yc\varphi_is\varphi_i-e_{ix})^2+(p_xc\varphi_is\varphi_i+p_ys^2\varphi_i-e_{iy})^2+(p_z-e_{iz})^2=0 \tag{12}$$

which is a system of three second-degree algebraic equations in the unknowns of $p_x$, $p_y$, and $p_z$.

***3.2.1 Forward Kinematics Solutions.*** The Sylvester dialytic elimination method is applied to reduce the system of Eq. (12) to an eighth-degree polynomial in only one variable.

First in order to eliminate $p_y$, writing Eq. (12) for $i=2$ and 3, respectively, into a second-degree polynomial in $p_y$

$$Ap_y^2+Bp_y+C=0 \tag{13}$$

$$Dp_y^2+Ep_y+F=0 \tag{14}$$

where $A$, $B$, $C$, $D$, $E$, and $F$ are all second-degree polynomials in $p_x$ and $p_z$.

Taking Eq. (14)$\times A$-Eq. (13) $\times D$ and Eq. (14)$\times C$-Eq. (13) $\times F$ respectively, and rewriting the two equations into the matrix form as

$$\begin{bmatrix} AE-BD & AF-CD \\ CD-AF & CE-BF \end{bmatrix}\begin{bmatrix} p_y \\ 1 \end{bmatrix}=\begin{bmatrix} 0 \\ 0 \end{bmatrix} \tag{15}$$

Equation (15) represents a system of two linear equations in $p_y$ and 1. The following equation can be obtained by equating the determinant of the coefficient matrix to zero:

$$(AE-BD)(CE-BF)+(AF-CD)^2=0 \tag{16}$$

Second for the purpose of eliminating $p_x$, we write Eq. (16) in the form of

$$Lp_x^4+Mp_x^3+Np_x^2+Pp_x+Q=0 \tag{17}$$

where $L$, $M$, $N$, $P$, and $Q$ can be shown to be second-degree polynomials in $p_z$

Substituting $\varphi_1=0$ deg into Eq. (12) for $i=1$, yields

$$(p_x-e_{1x})^2+e_{1y}^2+(p_z-e_{1z})^2=l^2 \tag{18}$$

which can be rewritten as

$$Gp_x^2+Hp_x+I=0 \tag{19}$$

where $G$, $H$, and $I$ are all second-degree polynomials in $p_z$

Now we can eliminate the unknown $p_x$ from Eqs. (17) and (19) as follows:

Taking Eq. (19)$\times Lp_x^2$-Eq. (17) $\times G$, we can obtain

$$(HL-GM)p_x^3+(IL-GN)p_x^2-GPp_x-GQ=0 \tag{20}$$

Taking Eq. (19)$\times(Lp_x^3+Mp_x^2)$-Eq. (17)$\times(Gp_x+H)$, yields

$$(GN-LI)p_x^3+(GP+HN-MI)p_x^2+(GQ+HP)p_x+HQ=0 \tag{21}$$

Multiplying Eq. (19) by $p_x$, we have

$$Gp_x^3+Hp_x^2+Ip_x=0 \tag{22}$$

Equations (19)–(22) can be considered as four linear homogeneous equations in the four variables of $p_x^3$, $p_x^2$, $p_x$, and 1. The characteristic determinant is

**Table 1 Architectural parameters of a 3-PRC TPM**

| Parameter | Value (m) | Parameter | Value (deg) |
|---|---|---|---|
| $a$ | 0.6 | $\alpha$ | 45 |
| $b$ | 0.3 | $\varphi_1$ | 0 |
| $l$ | 0.5 | $\varphi_2$ | 120 |
| $d_{\max}$ | 0.4 | $\varphi_3$ | 240 |
| $s_{\max}$ | 0.2 | | |

$$\begin{vmatrix} HL-GM & IL-GN & -GP & -GQ \\ GN-LI & GP+HN-MI & GQ+HP & HQ \\ G & H & I & 0 \\ 0 & G & H & I \end{vmatrix} = 0 \tag{23}$$

Expanding Eq. (23) results in an eighth-degree polynomial in $p_z$. It follows that there are at most eight solutions for $p_z$.

Once $p_z$ is found, $p_x$ and $p_y$ can be solved by using Eqs. (19) and (13) in sequence. There are total of 32 sets of solutions for $p_x$, $p_y$, and $p_z$.

Although the number of solutions is considerably large, it can be shown that only one solution is feasible and the preferred solution can be determined by examining the physical constrains of the mechanism.

***3.2.2 A Case Study***. In order to illustrate the derived forward kinematics solutions, an example is introduced to identify the configurations of the manipulator.

The architectural parameters of a 3-PRC TPM are described in Table 1. Assume that the actuated values are $d_1=0$, $d_2=0$, and $d_3=0$. Then, the polynomial of Eq. (23) becomes

$$2.8477z^8 + 4.3284z^6 + 1.9136z^4 + 0.0714z^2 - 0.0800 = 0 \tag{24}$$

which has eight solutions for $z$, and the solutions for $x$ and $y$ can be generated from Eqs. (19) and (13) in sequence, which are shown in Table 2, where the imaginary values of $z$ have no meanings, and the configurations with positive values of $p_z$ can only be implemented by resembling the mechanism. In addition, it is clear to see from the following Fig. 5 that configurations 2–4 do not lie in the range of the manipulator workspace subject to physical constraints imposed by stroke limits of C joints and motion limits of linear actuators. Thus, only configuration 1 stands for the real solution, and the unique feasible configuration is an important feature for real time control in robotic applications.

**Table 2 Forward kinematics solutions obtained via Sylvester dialytic elimination method**

| No. | $z$ (m) | $x$ (m) | $y$ (m) | Configuration |
|---|---|---|---|---|
| | | 0 | 0 | 1 |
| | | | 0.6928 | 2 |
| 1 | −0.4000 | 0.6000 | 0.3464 | 3 |
| | | | 1.0392 | 4 |
| 2 | 0.4000 | — | — | — |
| 3 | 0.7483$i$ | — | — | — |
| 4 | −0.7483$i$ | — | — | — |
| 5 | 0.7483$i$ | — | — | — |
| 6 | −0.7483$i$ | — | — | — |
| 7 | 0.7483$i$ | — | — | — |
| 8 | −0.7483$i$ | — | — | — |

## 4 Velocity Analysis

Substituting Eq. (5) into Eq. (4) and differentiating the result with respect to time, leads to

$$\dot{d}_i\mathbf{d}_{i0} = \dot{\mathbf{x}} - l\boldsymbol{\omega}_i \times \mathbf{l}_{i0} + \dot{s}_i\mathbf{s}_{i0} \tag{25}$$

where $\boldsymbol{\omega}_i$ is the vector of angular velocities for the $i$-th limb with respect to the fixed frame, and $\dot{\mathbf{x}}=[\dot{p}_x \quad \dot{p}_y \quad \dot{p}_z]^T$ denotes the vector of linear velocities for the mobile platform.

To eliminate the passive variable $\boldsymbol{\omega}_i$, we dot multiply both sides of Eq. (25) by $\mathbf{l}_{i0}$, this gives

$$\mathbf{l}_{i0}^T\mathbf{d}_{i0}\dot{d}_i = \mathbf{l}_{i0}^T\dot{\mathbf{x}} \tag{26}$$

Writing Eq. (26) three times, once for each $i=1$, 2, and 3, yields three scalar equations, which can be written into a matrix form

$$\mathbf{J}_q\dot{\mathbf{q}} = \mathbf{J}_x\dot{\mathbf{x}} \tag{27}$$

where

$$\mathbf{J}_q = \begin{bmatrix} \mathbf{l}_{10}^T\mathbf{d}_{10} & 0 & 0 \\ 0 & \mathbf{l}_{20}^T\mathbf{d}_{20} & 0 \\ 0 & 0 & \mathbf{l}_{30}^T\mathbf{d}_{30} \end{bmatrix}_{3\times3}, \quad \mathbf{J}_x = \begin{bmatrix} \mathbf{l}_{10}^T \\ \mathbf{l}_{20}^T \\ \mathbf{l}_{30}^T \end{bmatrix}_{3\times3} \tag{28}$$

and $\dot{\mathbf{q}}=[\dot{d}_1 \quad \dot{d}_2 \quad \dot{d}_3]^T$ is the vector of actuated joint rates.

When the manipulator is away from singularities, the following velocity equation can be derived from Eq. (27):

$$\dot{\mathbf{q}} = \mathbf{J}\dot{\mathbf{x}} \tag{29}$$

where

$$\mathbf{J} = \mathbf{J}_q^{-1}\mathbf{J}_x = \begin{bmatrix} \dfrac{\mathbf{l}_{10}^T}{\mathbf{l}_{10}^T\mathbf{d}_{10}} \\ \dfrac{\mathbf{l}_{20}^T}{\mathbf{l}_{20}^T\mathbf{d}_{20}} \\ \dfrac{\mathbf{l}_{30}^T}{\mathbf{l}_{30}^T\mathbf{d}_{30}} \end{bmatrix} = \begin{bmatrix} \mathbf{t}_1^T \\ \mathbf{t}_2^T \\ \mathbf{t}_3^T \end{bmatrix} \tag{30}$$

is defined as the Jacobian matrix of a 3-PRC TPM, which relates output velocities to the actuated joint rates.

## 5 Singular Configurations

Singular configurations are particular poses for the mobile platform of a parallel manipulator, in which the manipulator loses its inherent rigidity and the end effector has uncontrollable DOF, in other words, there exists an instantaneous gain or loss of DOF which results in a loss of the controllability of the manipulator. Therefore, the analysis of parallel manipulator singularities, which is necessary for both the design and control purposes, has drawn considerable attention [15–17]. In the following sections, all kinds of singular configurations are identified, and the mechanism design to eliminate them from the manipulator workspace is presented.

**5.1 Determination of Singular Configurations.** Four kinds of singularities can be derived for a 3-PRC TPM as follows:

(1) The first kind of singularity, which is also called the inverse kinematics singularity, occurs when $\mathbf{J}_q$ is not of full rank and $\mathbf{J}_x$ is invertible, i.e., $\det(\mathbf{J}_q)=0$ and $\det(\mathbf{J}_x)\neq0$.

From Eq. (28), we can see this is the case when $\mathbf{l}_{i0}^T\mathbf{d}_{i0}=0$ for $i=1$, 2, or 3, i.e., the direction of one or more legs are perpendicular to the axial directions of the corresponding actuated joints. In this situation, the mobile platform loses one or more DOF. Figure 4(*a*) illustrates an inverse kinematics singular configuration with link $C_1B_1$ perpendicular to $DA_1$ in the case of 0 deg $<\alpha<$ 90 deg. It is observed that link $C_1B_1$ is inclined

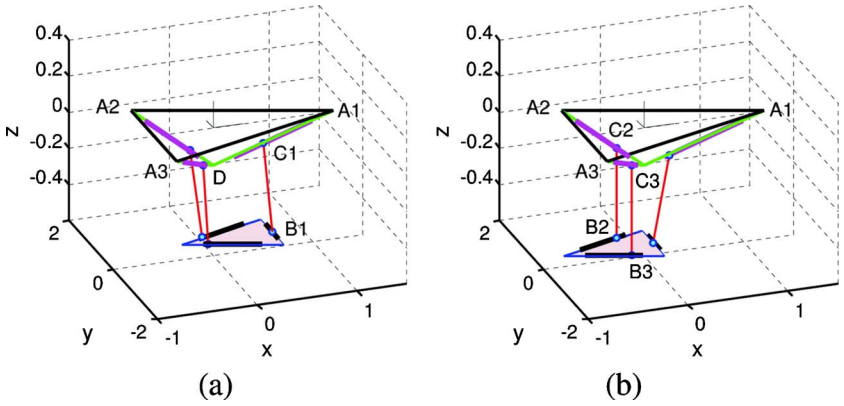


**Fig. 4 Representation of (*a*) inverse and (*b*) direct kinematics singular configurations for a 3-PRC TPM**

outward from top to bottom. Since only the configurations with the three legs being all inclined inward from top to bottom are selected in order to enhance the stiffness of the manipulator, this kind of singularity will not occur for the 3-PRC TPM in case of $0\ \text{deg} < \alpha < 90\ \text{deg}$.

(2) The second kind of singularity named the direct kinematics singularity occurs when $\mathbf{J}_x$ is not of full rank while $\mathbf{J}_q$ is invertible, i.e., $\det(\mathbf{J}_q) \neq 0$ and $\det(\mathbf{J}_x) = 0$.

From Eq. (28), we can deduce that it is the case when $\mathbf{l}_{i0}$, for $i=1$, 2, and 3, become linearly dependent. Physically, this type of singularity occurs when two or three of the legs are parallel to one another, or the three legs lie in a common plane. Under such cases, the manipulator gains one or more DOF even when all actuators are locked. One direct kinematics singular configuration is shown in Fig. 4(*b*), where links $B_2C_2$ and $B_3C_3$ are parallel to each other. With all actuators locked, the mobile platform still possesses an infinitesimal translation in the direction perpendicular to a plane defined by vectors $\mathbf{l}_{30}$ and $\mathbf{s}_{30}$.

(3) The third kind of singularity, which is also called the combined singularity, occurs when $\mathbf{J}_q$ and $\mathbf{J}_x$ become simultaneously not invertible, i.e., $\det(\mathbf{J}_q) = 0$ and $\det(\mathbf{J}_x) = 0$. Under this type of singularity, the mobile platform can undergo infinitesimal motions even when the actuators are locked, or equivalently, it cannot resist to forces or moments in one or more directions even if all actuators are locked. An infinitesimal motion of actuators gives no motion of the mobile platform.

This kind of singularity is architectural parameters dependent, and can only occur for a 3-PRC TPM when $\alpha = 0$ deg and $\|\overrightarrow{DC_i}\| = b$ with three vectors $\mathbf{l}_{i0}$ are all perpendicular to the base plane, or in the case of $\alpha = 90$ deg and $a = b + l$ with the three vectors $\mathbf{l}_{i0}$ locating on a common plane. Also notice that in the later case, the manipulator possesses a motion only along the $z$-axis direction.

(4) Besides the three types of singularities discussed above, the rotational singularity for a TPM may occur when the mobile platform of a TPM can rotate instantaneously [18]. This concept is generalized to the constraint singularity of limited-DOF parallel manipulators [19], and this type of singularity arises when the kinematic chains of a limited-DOF parallel manipulator cannot constrain the mobile platform to the planned motion any more. As far as a 3-PRC TPM is concerned, it is shown based on screw theory in Sec. 2 that the mobile platform cannot rotate at any instant, thus there are no rotational singularities for the 3-PRC TPM. Alternatively, it can be demonstrated more accurately via a mathematical method presented as follows, which is similar to that for a 3-RPC TPM [12].

Referring to Fig. 3, let $\mathbf{r}_{i0}$ and $\mathbf{c}_{i0}$ be the unit vectors for the axes of R and C joints of the $i$-th limb ($i=1,2,3$), respectively. In addition, let $\dot{\beta}_i$ and $\dot{\theta}_i$, respectively, denote the rotation rate of the R and C joints. The angular velocity $\boldsymbol{\omega}$ of the mobile platform can be expressed in terms of the joint velocities of each limb, i.e.,

$$\boldsymbol{\omega} = \dot{\beta}_i \mathbf{r}_{i0} + \dot{\theta}_i \mathbf{c}_{i0} \tag{31}$$

for $i=1$, 2, and 3.

In view of the geometric condition (i) mentioned in Sec. 2, i.e., $\mathbf{r}_{i0} = \mathbf{c}_{i0} = \mathbf{s}_{i0}$, Eq. (31) can be written into

$$\boldsymbol{\omega} = (\dot{\beta}_i + \dot{\theta}_i)\mathbf{s}_{i0} \tag{32}$$

Let $f_i = \dot{\beta}_i + \dot{\theta}_i$, then Eq. (32) can be rewritten as

$$\boldsymbol{\omega} = f_i \mathbf{s}_{i0} \tag{33}$$

Subtracting Eq. (33) for $i=1$ from Eq. (33) for $i=2$, Eq. (33) for $i=2$ from Eq. (33) for $i=3$, and Eq. (33) for $i=3$ from Eq. (33) for $i=1$, respectively, allows the derivation of a system of three linear equations, which can be rewritten into a matrix form

$$\mathbf{Sf} = \mathbf{0} \tag{34}$$

where

$$\mathbf{S} = \begin{bmatrix} -\mathbf{s}_{10} & \mathbf{s}_{20} & 0 \\ 0 & -\mathbf{s}_{20} & \mathbf{s}_{30} \\ \mathbf{s}_{10} & 0 & -\mathbf{s}_{30} \end{bmatrix}_{9\times 3}, \quad \mathbf{f} = \begin{bmatrix} f_1 \\ f_2 \\ f_3 \end{bmatrix}_{3\times 1}, \quad \mathbf{0} = \begin{bmatrix} 0 \\ \vdots \\ 0 \end{bmatrix}_{9\times 1}$$

Due to the geometric condition (ii) described in Sec. 2, matrix $\mathbf{S}$ always has a full rank, then the only solution to the homogeneous system of Eq. (34) is $\mathbf{f}=\mathbf{0}$, and consequently, $f_i=0$ for $i=1$, 2, and 3. In view of Eq. (33), we have

$$\boldsymbol{\omega} = \mathbf{0} \tag{35}$$

Moreover, differentiating Eq. (31) with respect to time and in view of $\dot{\mathbf{s}}_{i0}=0$ since $\mathbf{s}_{i0}$ is a constant unit vector, allows the generation of the angular acceleration $\dot{\boldsymbol{\omega}}$ of the mobile platform, i.e.,

$$\dot{\boldsymbol{\omega}} = (\ddot{\beta}_i + \ddot{\theta}_i)\mathbf{s}_{i0} \tag{36}$$

In the same way, it can be shown that the following result holds as well with the geometric conditions (i) and (ii) satisfied:

$$\dot{\boldsymbol{\omega}} = \mathbf{0} \tag{37}$$

It can be deduced from Eqs. (35) and (37) that, satisfying the two geometric conditions, a 3-PRC parallel manipulator acts as a translational parallel manipulator all the time. Therefore, no constraint singularities can occur for the 3-PRC TPM.

**5.2 Mechanism Design to Eliminate Singularities.** The singular configurations can be eliminated by the approach of mechanism design as follows:

(1) Elimination of the direct kinematics singularities: According to the aforementioned analysis, three cases can be classified for the direct kinematics singularity.

Case I—two legs are parallel to each other. Assume that $\mathbf{l}_{10}$ is parallel to $\mathbf{l}_{20}$. For simplicity, let the 3-PRC TPM possess a symmetric architecture. It can be deduced that $\mathbf{l}_{10}$ and $\mathbf{l}_{20}$ are perpendicular to the base plane. Generating $\mathbf{s}_{10}$ and $\mathbf{p}$, and substituting them into Eq. (7) for $i=1$, allows the generation of $s_1=\sqrt{3}(a-b-d_1c\alpha)$, where $d_1=d_2$. With the consideration of Eq. (3), the maximum stroke of C joints should be designed as

$$s_{\max} < 2\sqrt{3}\left(a-b-\frac{d_{\max}}{2}c\alpha\right) \tag{38}$$

in order to eliminate this kind of singular configurations.

Case II—the three legs are parallel to one another. Under such a case, it is seen that the three vectors $\mathbf{l}_{10}$, for $i=1$, 2, and 3, are all perpendicular to the base plane. In addition, $d_1=d_2=d_3$ and $b=a-d_1c\alpha$. To eliminate this singularity, the maximum stroke of linear actuators should be designed as

$$d_{\max} < 2d_1 = \frac{2(a-b)}{c\alpha}, \quad \text{if} \quad \alpha \neq 90 \text{ deg} \tag{39}$$

Case III—the three legs lie in a common plane. In this situation, the three vectors $\mathbf{l}_{10}$ lie in a plane parallel to the base plane. It can be deduced that $d_1=d_2=d_3$ and $b+l=a\pm d_1c\alpha$. To eliminate this singularity, the maximum stroke of linear actuators should be designed as

$$d_{\max} < 2d_1 = \frac{2\|a-b-l\|}{c\alpha}, \quad \text{if} \quad \alpha \neq 90 \text{ deg} \tag{40}$$

(2) Elimination of the combined singularities: From the above discussions, we can see that the combined singularity occurs in the cases of $\alpha=0$ deg with $d_1=d_2=d_3=a-b$, or $\alpha=90$ deg with $a=b+l$. Thus, we can eliminate this type of singularities by the design of

$$d_{\max} < 2(a-b), \quad \text{if} \quad \alpha = 0 \text{ deg} \tag{41}$$

$$a < b+l, \quad \text{if} \quad \alpha = 90 \text{ deg} \tag{42}$$

Therefore, in a real machine design, Eqs. (38)–(42) should be satisfied at the same time so as to eliminate all singular configurations from the workspace of a 3-PRC TPM.

## 6 Isotropic Configurations

An isotropic manipulator is a manipulator with the Jacobian matrix having a condition number equal to 1 in at least one of its configurations. In isotropic configurations, the manipulator performs very well with regard to the force and velocity transmission. As for a 3-PRC TPM in isotropic configurations, the Jocobian matrix $\mathbf{J}$ should satisfy

$$\mathbf{J}\mathbf{J}^T = \sigma\mathbf{I}_{3\times 3} \tag{43}$$

where $\mathbf{I}_{3\times 3}$ is the $3\times 3$ identity matrix. Under such a case, in view of Eq. (30), the following conditions need to hold:

$$\sigma = \mathbf{t}_i^T\mathbf{t}_i = 1 \tag{44}$$

$$\mathbf{t}_i^T\mathbf{t}_j = 0 \quad \text{for} \quad i \neq j \tag{45}$$

for $i,j=1$, 2, and 3.

From Eq. (45), we can see that the three vectors $\mathbf{t}_i$ are perpendicular to one another. Writing Eq. (44) three times, once for each $i=1$, 2, and 3, respectively, results in three equations in the unknowns of $p_x$, $p_y$, and $p_z$. Solving them, allows the generation of isotropic configurations. Given the symmetric architecture of a 3-PRC TPM, the isotropic configurations, which lie along the $z$ axis, can be derived by

$$\mathbf{p} = \left[0 \quad 0 \quad -ds\alpha \pm \frac{\sqrt{2}}{2}(a-b-dc\alpha)\right]^T \tag{46}$$

where $d=d_1=d_2=d_3$. Only the negative sign is taken into consideration since we are interested only in the point below the actuators.

Moreover, under such a case, the relationship between architectural parameters can be derived through a careful analysis, i.e.,

$$l = \frac{\sqrt{6}}{2}(a-b-dc\alpha) \tag{47}$$

Deriving $d$ from Eq. (47) and in view of Eq. (2), allows the generation of

$$\begin{cases} -\dfrac{d_{\max}}{2} \leqslant \dfrac{a-b-\dfrac{\sqrt{6}}{3}l}{c\alpha} \leqslant \dfrac{d_{\max}}{2} & \text{if} \quad \alpha \neq 90 \text{ deg} \\ a-b = \dfrac{\sqrt{6}}{3}l & \text{if} \quad \alpha = 90 \text{ deg} \end{cases} \tag{48}$$

which are the isotropy conditions resulting in an isotropic 3-PRC TPM.

## 7 Workspace Analysis

It is well known that compared with their serial counterparts, parallel manipulators have relatively small workspaces. Thus the workspace of a parallel manipulator is one of the most important aspects to reflect its working capacity, and it is necessary to analyze the shape and volume of the workspace for enhancing applications of parallel manipulators [20,21]. Furthermore, for a real machine design, it is of particular interest to determine how the workspace varies with different values of the architectural parameters. The reachable workspace of a 3-PRC TPM presented here is defined as the space that can be reached by the reference point $P$.

**7.1 Algorithms.** Equation (12) represents the workspace of the $i$-th ($i=1,2,3$) limb, which is a set of cylinders with the radii of $l$. The manipulator workspace can be derived geometrically by the intersection of the three limbs' workspace. From the easily derived result, it is observed that there exists no void within the workspace, i.e., the cross section of the workspace is consecutive at every height. This allows the use of a numerical search method in cylindrical coordinates by slicing the workspace into a series of subworkspaces [8], and the boundary of each subworkspace is successively determined based on the inverse kinematics solutions along with the physical constraints taken into consideration. The total workspace volume is approximately calculated as the sum of these subworkspaces. The adopted numerical approach can facilitate the dexterity analysis of the manipulator discussed later.

**7.2 A Case Study.** The architectural parameters of a 3-PRC TPM shown in Table 1 have been designed so as to eliminate all of the singular configurations from the workspace and also to generate an isotropic manipulator. Calculating $d$ from Eq. (47), and substituting it into Eq. (46), allows the derivation of the isotropic configuration, i.e., $\mathbf{p}=[0 \quad 0 \quad -0.1804]^T$.

The workspace of the manipulator is generated by a developed MATLAB program and illustrated in Fig. 5, where the isotropic

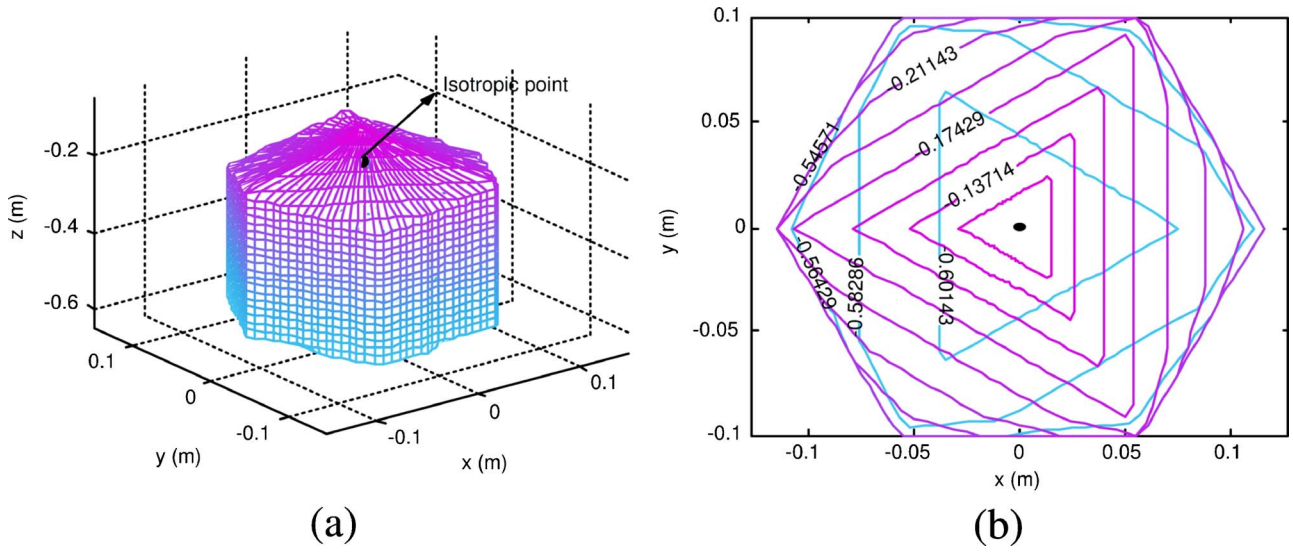


**Fig. 5 Reachable workspace of a 3-PRC TPM: (*a*) three-dimensional view; (*b*) *x-y* section at different heights**

point is also indicated. It is observed that the reachable workspace is 120 deg symmetrical about the three motion directions of actuators from overlook, and can be divided into the upper, middle, and lower parts. In the minor upper and lower parts of the workspace, the cross sections have a triangular shape. While in the definitive major middle range of the workspace, most of the applications will be performed, it is of interest to notice that the proposed manipulator has a uniform workspace without variation of the cross-sectional area which takes on the shape of a hexagon.

Additionally, it is necessary to identify the impact on the workspace with the variation of architecture parameters. For the aforementioned 3-PRC TPM, with the varying of mobile platform size ($b$), the simulation results of the workspace volumes are shown in Fig. 6, which illustrates that the maximum workspace size occurs when $b=0.2$. However, in view of Eqs. (38)–(42), it can be verified that there exist singularities when $b$ has the value of 0.1 m, 0.2 m, 0.4 m, or 0.5 m, etc. In addition, Fig. 7 describes the variation tendency of workspace size as the increasing of actuator layout angle. It is observed that the maximum workspace volume occurs when $\alpha$ is around 45 deg. It can be shown that there exist no singular configurations along with the varying of $\alpha$, but the manipulator possesses no isotropic configurations if $\alpha > 57.2$ deg. The simulation results reveal the roles of conditions expressed by Eqs. (38)–(42) and (48) in designing a 3-PRC TPM.

## 8 Dexterity Analysis

Dexterity is an important issue for design, trajectory planning, and control of manipulators, and has emerged as a measure for manipulator kinematic performance [22]. The dexterity of a manipulator can be thought as the ability of the manipulator to arbitrarily change its position and orientation, or apply forces and torques in arbitrary directions. In this section, we focus on discovering the dexterity characteristics of a 3-PRC TPM in a local sense and global sense, respectively.

**8.1 Dexterity Indices.** In literatures, different indices of manipulator dexterity are introduced. One of the frequently used indices is called kinematic manipulability expressed by the square root of the determinant of $\mathbf{JJ}^T$

$$\omega = \sqrt{\det(\mathbf{JJ}^T)} \tag{49}$$

Since the Jacobian matrix ($\mathbf{J}$) is configuration dependent, kinematic manipulability is a local performance measure, which also gives an indication of how close the manipulator is to the singularity. For instance, $\omega=0$ means a singular configuration, and therefore we wish to maximize the manipulability index to avoid singularities.

Another usually used index is the condition number of Jacobian matrix. As a measure of dexterity, the condition number ranges in value from one (isotropy) to infinity (singularity) and thus mea-

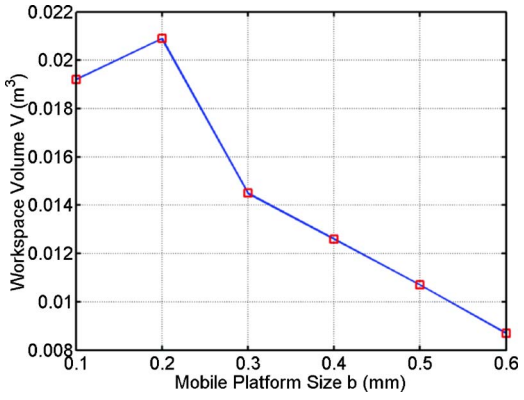


**Fig. 6 Workspace volume versus mobile platform size**

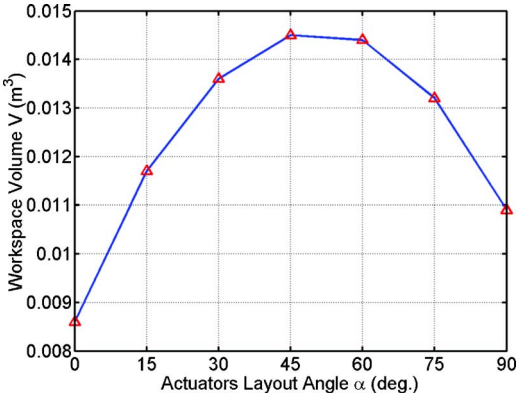


**Fig. 7 Workspace volume versus actuators layout angle**

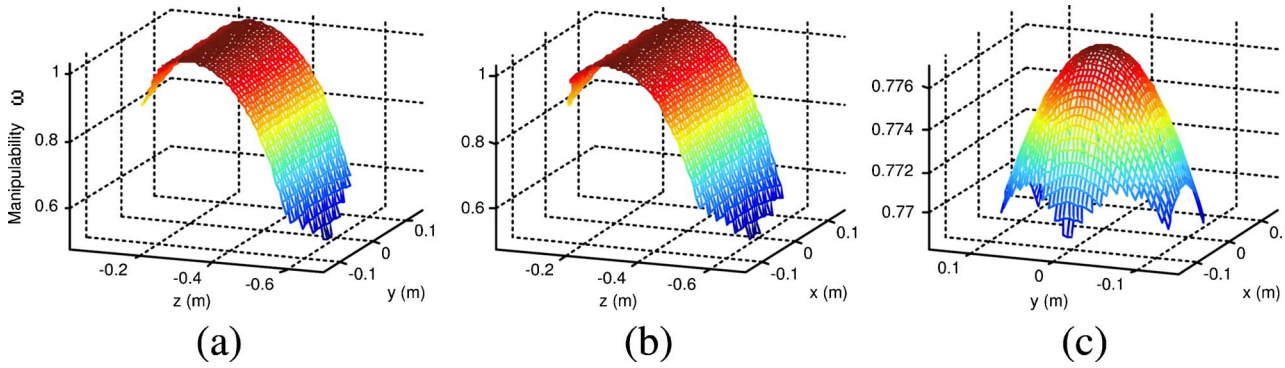


**Fig. 8 Manipulability distribution of a 3-PRC TPM in three planes of (*a*) *x*=0, (*b*) *y*=0, and (*c*) *z*=−0.5 m**

sures the degree of ill conditioning of the Jacobian matrix, i.e., nearness of the singularity, and it is also a local measure dependent solely on the configuration, based on which a global dexterity index (GDI) is proposed in [23] as follows:

$$\mathrm{GDI} = \frac{\int_V \left(\frac{1}{\kappa}\right) dV}{V} \tag{50}$$

where $V$ is the total workspace volume, and $\kappa$ denotes the condition number of the Jacobian and can be defined as $\kappa = \|\mathbf{J}\|\|\mathbf{J}^{-1}\|$, with $\|\bullet\|$ denotes the two-norm of the matrix. Moreover, the GDI represents the uniformity of dexterity over the entire workspace other than the dexterity at a certain configuration, and can give a measure of kinematic performance independent of the different workspace volumes of the design candidates since it is normalized by the workspace size.

### 8.2 Case Studies.

***8.2.1 Kinematic Manipulability***. Regarding a 3-PRC TPM, since it is a nonredundant manipulator, manipulability measure $\omega$ reduces to

$$\omega = |\det(\mathbf{J})| \tag{51}$$

With actuators layout angle $\alpha$=30 deg and other parameters as described in Table 1, the manipulability of a 3-PRC TPM in the planes of $x$=0, $y$=0, and $z$=−0.5 m are shown in Fig. 8. It can be observed from Figs. 8(*a*) and 8(*b*) that in $y$-$z$ and $x$-$z$ planes, manipulability is maximal when the center point of the mobile platform lies in the $z$ axis and at the height of the isotropic point, and decreases when the mobile platform is far from the $z$ axis and away from the isotropic point. From Fig. 8(*c*), it is seen that in a plane at certain height, manipulability is maximal when the mobile platform lies along the $z$ axis, and decreases in case of the manipulator approaching to its workspace boundary.

***8.2.2 Global Dexterity Index (GDI)***. Because there exist no closed-form solutions for Eq. (50), the integral of the dexterity must be calculated numerically, which can be approximated by a discrete sum

$$\mathrm{GDI} \approx \frac{1}{N_w} \sum_{w \in V} \frac{1}{\kappa} \tag{52}$$

where $w$ is one of $N_w$ points which are uniformly distributed over the entire workspace of the manipulator.

Figures 9(*a*) to 9(*c*), respectively, illustrate the distribution of the reciprocal of Jacobian matrix condition number in three planes of $x$=0, $y$=0, and $z$=−0.5 m for a 3-PRC TPM with $\alpha$=30 deg and other parameters depicted in Table 1. It is observed that the figures show the similar yet sharper tendencies of changes than those described in Fig. 8.

With the changing of layout angle of actuators, we can calculate the GDI of the 3-PRC TPM over the entire workspace, and the simulation results are shown in Fig. 10. It can be observed that the maximum value of GDI occurs when $\alpha$=0 deg, and decreases along with the increasing of layout angle of actuators. However, in the case of $\alpha$=0 deg, it is seen from Fig. 7 that the workspace volume is relatively small. Since the selection of a manipulator depends heavily on the task to be performed, different objectives should be taken into account when the actuators layout angle of a 3-PRC TPM is designed, or alternatively, several required performance indices may be considered simultaneously.

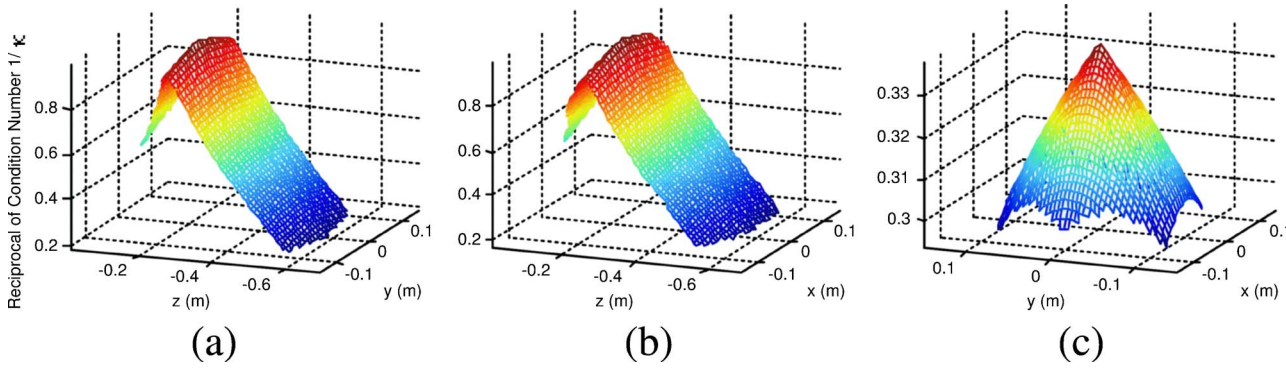


**Fig. 9 Distribution of reciprocal of the Jacobian matrix condition number for a 3-PRC TPM in three planes of (*a*) *x*=0, (*b*) *y*=0, and (*c*) *z*=−0.5 m**

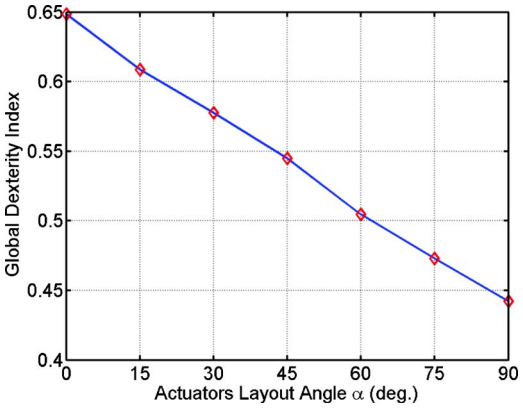


**Fig. 10 Global dexterity index versus actuators layout angle**

## 9 Conclusions

In this paper, a novel 3-PRC TPM with fixed actuators has been proposed. It is shown that such a mechanism can act as an overconstrained 3-DOF TPM with certain assembling conditions satisfied. The closed-form solutions for both the inverse and forward kinematics problems have been derived, and the velocity analysis is performed, where the Jacobian matrix relating output velocities to the actuated joint rates has been derived, based on which the isotropic configurations and three kinds of singularities having been identified. Moreover, it is demonstrated that the new TPM does not exhibit rotational singularities, i.e., the configurations in which the mobile platform gains rotational DOF. In addition, an approach to eliminate all singularities by a proper design of architectural parameters is proposed, and the isotropy conditions leads to an isotropic manipulator have been derived.

The reachable workspace of the manipulator is generated by a numerical approach, which illustrates that in the middle range of the workspace in which most practical applications will be performed, the cross section takes on a constant hexagon shape. Furthermore, the workspace volume is calculated and compared at different mobile platform sizes and actuator layout angles. With the variation on actuator layout angle, dexterity characteristics of the manipulator are investigated based on a local performance measure—kinematic manipulability, and a global sense measure—global dexterity index over the entire workspace, respectively. Simulation results illustrate that different objectives should be taken into consideration when the actuators layout angle of a 3-PRC TPM is designed.

In addition, as an overconstrained mechanism, the problems of variable friction in passive joints and large reaction moment have to be considered to assure the mobility of the mobile platform for a 3-PRC TPM. Otherwise, the mobile platform may not move or the manipulator cannot work if there are some kinematic errors. These issues can be solved by adding a revolute joint with its axis along the axial direction of the first actuated prismatic joint, thus the actual structure of limbs becomes a PRRC mechanism. This design choice results in a nonoverconstrained manipulator and causes no impact on the mobility and kinematics of the manipulator. The results presented in this paper will be valuable in the development of a new TPM.

## Acknowledgment

The authors appreciate the fund support from the research committee of the University of Macau under Grant No. RG083/04-05S/LYM/FST. The authors also appreciate very much the comments and suggestions from anonymous reviewers and the editor.

## References

[1] Merlet, J.-P., 2000, *Parallel Robots*, Kluwer Academic Publishers, London.
[2] Su, H.-J., Dietmaier, P., and McCarthy, J. M., 2003, "Trajectory Planning for Constrained Parallel Manipulators," ASME J. Mech. Des., **125**(4), pp. 709–716.
[3] Angeles, J., 2004, "The Qualitative Synthesis of Parallel Manipulators," ASME J. Mech. Des., **126**(4), pp. 617–624.
[4] Huang, Z., and Li, Q. C., 2003, "Type Synthesis of Symmetrical Lower-Mobility Parallel Mechanisms Using the Constraint-Synthesis Method," Int. J. Robot. Res., **22**(1), pp. 59–79.
[5] Li, Y., and Xu, Q., 2005, "Dynamic Analysis of a Modified DELTA Parallel Robot for Cardiopulmonary Resuscitation," *Proceedings of IEEE/RSJ International Conference on Intelligent Robots and Systems*, Edmonton, Canada, August 2-6, pp. 3371–3376.
[6] Chablat, D., and Wenger, P., 2003, "Architecture Optimization of a 3-DOF Translational Parallel Mechanism for Machining Applications, the Orthoglide," IEEE Trans. Rob. Autom., **19**(3), pp. 403–410.
[7] Carretero, J. A., Podhorodeski, R. P., Nahon, M. A., and Gosselin, C. M., 2000, "Kinematic Analysis and Optimization of a New Three Degree-of-Freedom Spatial Parallel Manipulator," ASME J. Mech. Des., **122**(1), pp. 17–24.
[8] Li, Y., and Xu, Q., 2004, "Kinematics and Stiffness Analysis for a General 3-PRS Spatial Parallel Mechanism," *Proceedings of 15th CISM-IFToMM Symposium on Robot Design, Dynamics and Control*, Montreal, Canada, June 14-18, Rom 04–15.
[9] Li, Y., and Xu, Q., 2005, "Kinematics and Inverse Dynamics Analysis for a General 3-PRS Spatial Parallel Mechanism," Robotica, **23**(2), pp. 219–229.
[10] Tsai, L. W., and Joshi, S., 2000, "Kinematics and Optimization of a Spatial 3-UPU Parallel Manipulator," ASME J. Mech. Des., **122**(4), pp. 439–446.
[11] Tsai, L. W., and Joshi, S., 2002, "Kinematics Analysis of 3-DOF Position Mechanisms for Use in Hybrid Kinematic Machines," ASME J. Mech. Des., **124**(2), pp. 245–253.
[12] Callegari, M., and Tarantini, M., 2003, "Kinematic Analysis of a Novel Translational Platform," ASME J. Mech. Des., **125**(2), pp. 308–315.
[13] Kong, X., and Gosselin, C. M., 2002, "Kinematics and Singularity Analysis of a Novel Type of 3-CRR 3-DOF Translational Parallel Manipulator," Int. J. Robot. Res., **21**(9), pp. 791–798.
[14] Kim, H. S., and Tsai, L. W., 2003, "Design Optimization of a Cartesian Parallel Manipulator," ASME J. Mech. Des., **125**(1), pp. 43–51.
[15] Wang, J., and Gosselin, C. M., 2004, "Kinematic Analysis and Design of Kinematically Redundant Parallel Mechanisms," ASME J. Mech. Des., **126**(1), pp. 109–118.
[16] Di Gregorio, R., 2004, "Forward Problem Singularities of Manipulators Which Become PS-2RS or 2PS-RS Structures When the Actuators are Locked," ASME J. Mech. Des., **126**(4), pp. 640–645.
[17] Liu, C. H., and Cheng, S., 2004, "Direct Singular Positions of 3RPS Parallel Manipulators," ASME J. Mech. Des., **126**(6), pp. 1006–1016.
[18] Di Gregorio, R., and Parenti-Castelli, V., 1999, "Mobility Analysis of the 3-UPU Parallel Mechanism Assembled for a Pure Translational Motion," *Proceedings of IEEE/ASME International Conference on Advanced Intelligent Mechatronics*, Atlanta, Georgia, Sept. 19-23, pp. 520–525.
[19] Zlatanov, D., Bonev, I. A., and Gosselin, C. M., 2002, "Constraint Singularities of Parallel Mechanisms," *Proceedings of IEEE International Conference on Robotics and Automation*, Washington, DC, May 11-15, pp. 496–502.
[20] Li, Y., and Xu, Q., 2005, "Kinematic Analysis of a New 3-DOF Translational Parallel Manipulator," *Proceedings of ASME 2005 International Design Engineering Technical Conferences and Computers and Information in Engineering Conference, DETC2005-84299*, Long Beach, California, Sept. 24-28, DETC2005-84299.
[21] Li, Y., and Xu, Q., 2005, "Kinematic Design of a Novel 3-DOF Compliant Parallel Manipulator for Nanomanipulation," *Proceedings of IEEE/ASME International Conference on Advanced Intelligent Mechatronics*, pp. 93–98.
[22] Li, Y., and Xu, Q., 2005, "Kinematics and Dexterity Analysis for a Novel 3-DOF Translational Parallel Manipulator," *Proceedings of IEEE International Conference on Robotics and Automation*, Barcelona, Spain, April 18–22, pp. 2955–2960.
[23] Gosselin, C., and Angeles, J., 1991, "A Global Performance Index for the Kinematic Optimization of Robotic Manipulators," ASME J. Mech. Des., **113**(3), pp. 220–226.